ADVANCED MATERIALS

Supporting Information

for *Adv. Mater.*, DOI: 10.1002/adma.201203021

Piezoelectric-Polarization-Enhanced Photovoltaic Performance in Depleted-Heterojunction Quantum-Dot Solar Cells

*Jian Shi, Ping Zhao, and Xudong Wang**

Supporting Information

Piezoelectric Polarization Enhanced Photovoltaic Performance in Depleted Heterojunction Quantum Dot Solar Cells

By *Jian Shi, Ping Zhao, Xudong Wang**

[*] Prof. X. Wang, J. Shi, P. Zhao
Department of Materials Science and Engineering, University of Wisconsin-Madison, Madison, WI 53706, USA
Email: xudong@engr.wisc.edu

S1. Layout of DHSC

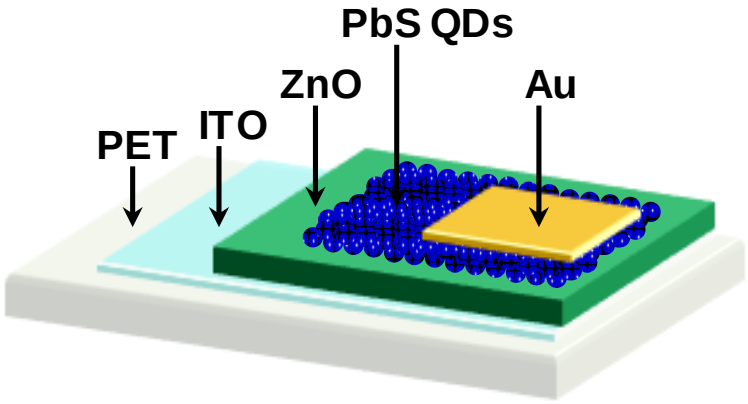

Figure S1. Schematic layout of depleted heterojunction quantum dots solar cell

S2. Estimation of Screening Potential by PbS

In a sandwiched "electrode I/semiconducting ZnO/electrode II" structure, free charges that screen the piezoelectric polarization (P_{pz}) usually come from all the three components. The detectable piezoelectric potential is corresponding to the amount of charges that flow through the external circuit driven by the screening charge redistribution. Therefore, the amplitude of piezoelectric potential spikes can be used to estimate the amount of screening charge that accumulated at the ZnO/electrode interface in response to the appearance of P_{pz}. Typically, due to the very high electron concentration, metal electrodes can almost fully screen P_{pz} within a very small thickness (a fraction of angstrom).[1] Therefore, the piezoelectric potential measured from Au/ZnO/Au configuration (red circles in Fig. S2a) represent almost the maximum amount of charge that can be redistributed externally. When PbS layer was directly applied to the ZnO

surface, the detected piezoelectric potential (blue squares in Fig. S2a) was significantly smaller due to its limited intrinsic free charge carrier concentration. Because the detected piezoelectric potentials are equivalent to the potential change due to charge redistribution at the ZnO/PbS interface,[2] this potential-strain relationship can represent the P_{pz}-induced built-in potential change at the ZnO/PbS interface. The amplitude of the potential change (~0.13 V per 0.1% strain) was comparable to the space charge-induced built-in potential (~0.6 V) and thus a significant influence toward the ZnO/PbS interface band structure can be expected.

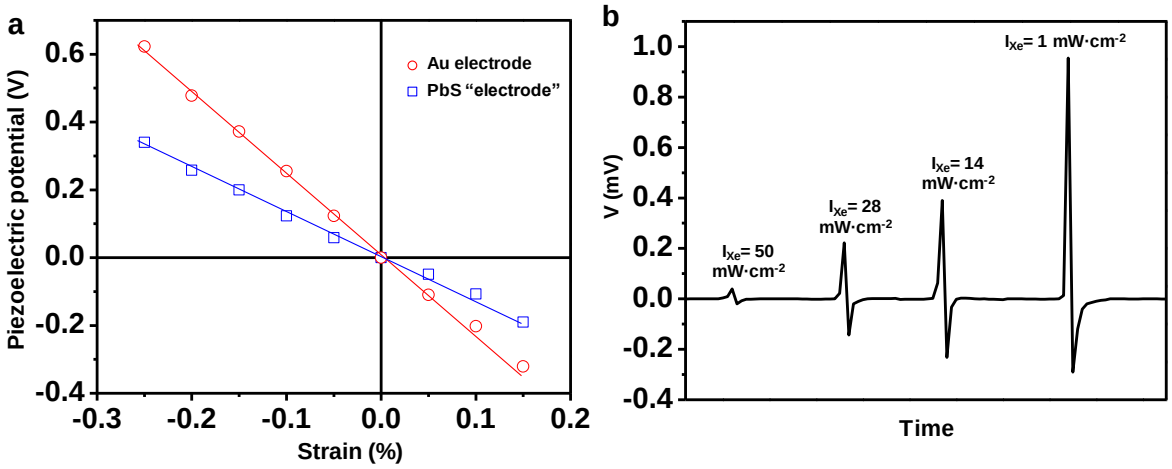

Figure S2. A. Relation between piezoelectric potential and mechanical strain when Au and PbS served as screening electrodes, respectively. Thickness of ZnO film was 200 nm. **B**. Piezoelectric response of a 500 nm ZnO film with ITO and Ag as electrodes under different light intensities.

Under illumination, when photoexcited charges could not be promptly swept away from the ZnO/electrode interface, photoexcited charges can participate into the screening process, which could be very significant especially when a high density of surface/interface trapping states exists.[3] Figure 2b gives the piezoelectric response of ITO/ZnO/Ag structure under different intensities of illumination. It illustrates that a strong illumination can dramatically suppress the detectable piezoelectric potential from ZnO due to a large quantity of photoexcited free charges. If these free charges interact with the interface states, they will screen P_{pz} locally. Thus, the P_{pz}-induced intrinsic charge redistribution near the interface will be diminished, so that the depletion region change will be less. This is the reason that much more pronounced PV efficiency change was observed at very low illumination intensity. This mechanism also suggests that if the heterogeneous interface has very high quality and free of defects, the P_{pz} modulation effect could remain significant even under high illumination intensity.

S3. Internal Impedance of QDSC Characterized by EIS

To rule out the possibility that photocurrent density change subject to mechanical strains comes from the response of abnormal interface in QDSC, EIS measurements were conducted under forward bias of 0.6 V and 0.5 V at a frequency range of 1 MHz to 0.1Hz. Figure S3 demonstrates the Nyquist plots of internal impedance, which exhibited a typical spectrum as good quality QDSCs, excluding the existing of erratic interfaces. The low series resistance of cell

at applied bias of 0.6 V (close to its open circuit voltage) at low frequency range indicates that the impedance at ZnO-PbS interface is rather low.

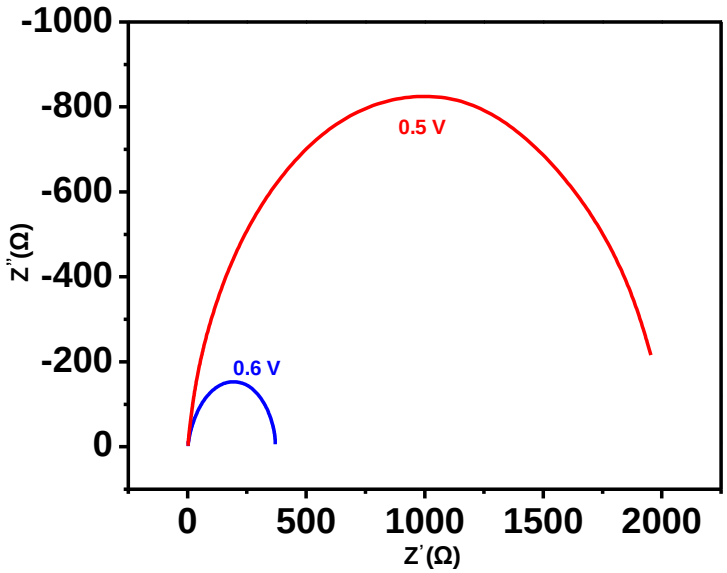

Figure S3. Nyquist plots from the EIS measurements in the dark at forward biases.

The capacitance of the anisotype heterojunction under reverse bias *via* equation:[4]

$$C^{-1} = C_{ZnO}^{-1} + C_{PbS}^{-1} = \frac{\delta_{pz,ZnO}}{\varepsilon_{ZnO}} + \frac{\delta_{pz,PbS}}{\varepsilon_{PbS}} =$$

$$\sqrt{\frac{2(-V_{ZnO}+\varphi_{bi,ZnO} \mp \Delta\varphi_{pz,ZnO})}{q\varepsilon_{ZnO}N_{ZnO,eff}}} + \sqrt{\frac{2(-V_{PbS}+\varphi_{bi,PbS} \pm \Delta\varphi_{pz,PbS})}{q\varepsilon_{PbS}N_{PbS,eff}}}. \quad (1)$$

Here, V_{ZnO} and V_{PbS} are externally applied bias shared between ZnO and PbS, respectively, which, theoretically, has equivalent contribution to C as P_{pz}-induced built-in potential change ($\Delta\varphi_{pz,ZnO}$ and $\Delta\varphi_{pz,PbS}$). $\delta_{pz,PbS}$ and $\delta_{pz,ZnO}$ are the widths of depletion regions in PbS and ZnO, respectively. According to equation (3), a positive P_{pz} can yield a reduced depletion region on the ZnO side (C_{ZnO} increases) but an extended depletion region on the PbS side (C_{PbS} decreases). Therefore, under positive P_{pz}, a decreased C is a result of the extended depletion region in PbS.

The change of depletion region can be determined by equation:[4]

$$\frac{\Delta\delta}{\delta} = \sqrt{\frac{V_{pz,PbS}+V_{bi,PbS}}{V_{bi,PbS}}} - 1. \quad (2)$$

And the built-in potential shared in PbS assemblage can be calculated by:[4]

$$\frac{V_{bi,PbS}}{V_{bi}} = \frac{\varepsilon_{ZnO}N_{ZnO}}{\varepsilon_{ZnO}N_{ZnO}+\varepsilon_{PbS}N_{PbS}}. \quad (3)$$

Upon 30 minutes UV photo-doping prior to electrical characterization, N_{ZnO} is a few orders higher than N_{PbS}.[5] Besides, ε_{ZnO} (8.5) has the similar scale as ε_{PbS} (14.5).[6][7] Therefore, $V_{bi,PbS}$

here can be simply regarded as the V_{oc} (for instance, 0.435 V for the cells shown in Figure 2a and 2c with QDs of absorption edge at 1500 nm) of QDSC.[5]

S4. Pronounced Piezotronics Effect of Thick-ZnO-Layer QDSC

The diffusion length of ZnO film in a depletion heterojunction QDSC was reported to be ~ 200 nm, which legitimates the thickness of ZnO to be around 200 nm.[6] However, equivalent surface charge of P_{pz} is proportional to the thickness of ZnO film under the same strain. Thus, a more pronounced built-in potential/depletion region change in the PbS layer could be expected by straining thicker ZnO films, which could trigger a more prominent PV efficiency change in QDSCs. To exaggerate such effects, a 920 nm thick ZnO layer was applied in QDSC fabrication and all the other parameters were kept consistent with the 200 nm ones. The piezoelectric potential was measured as shown in Figure S4, which illustrated an approximate 5 times higher P_{pz}-induced built-in potential change compared to the 200 nm ZnO QDSCs. Under 0.0047 mW/cm^2 illumination, photocurrent and PV efficiency changes of such QDSCs have been characterized and demonstrated in Fig. S5. Overall performance of the cell was inferior to the 200 nm ones due to the over thick ZnO layer that jeopardized charge transport. However, owing to the larger piezoelectric potential, the photocurrent density and efficiency increases have reached ~90% and ~144%, respectively, under a compressive strain of -0.25%, which was much higher than the 200 nm-ZnO QDSCs. This observation suggested that the P_{pz} modulation could be tremendous when a piezoelectric current collector material with high electron mobility and large electrochemical coupling can be achieved.

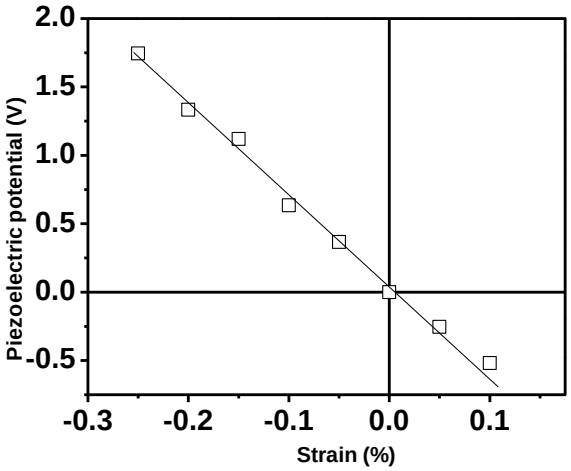

Figure S4. Relation between piezoelectric potential and mechanical strain when PbS served as screening electrode. Thickness of the ZnO film was 920 nm.

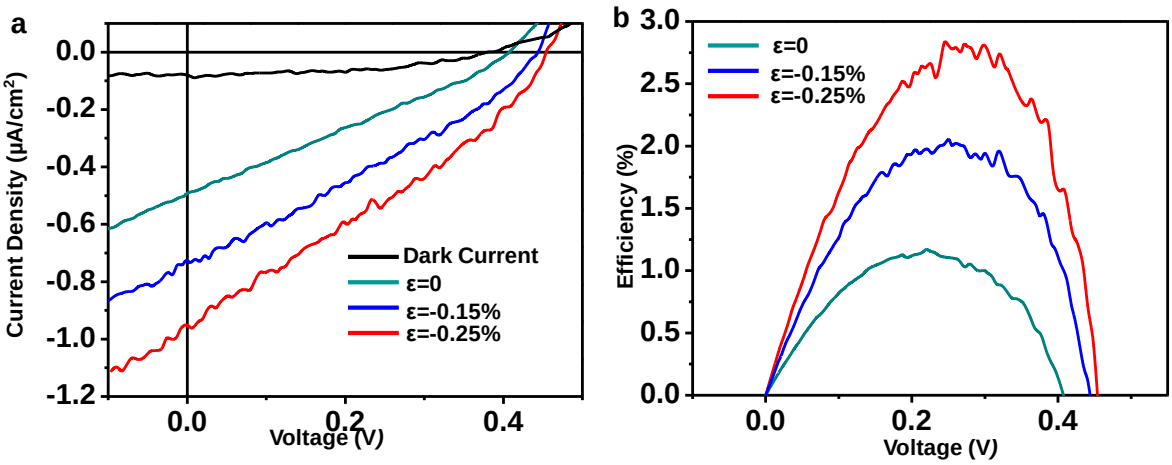

Figure S5. J-V characteristics **a.** and corresponding efficiencies **b.** of a ZnO/PbS QDSC under different compressive strains. Thickness of the ZnO film was 920 nm.

S5. Constant Open Circuit Voltage Change under Strains

Potentiostat measurement was conducted to confirm that the change of open circuit voltage (V_{oc}) of QDSC was permanent under constant strains (Fig. S6). Figure S6a demonstrates that a compressive strain of -0.15% produced a ~7.5 mV consistent and stable V_{oc} increase under illumination intensity of 25 mW/cm^2. An equal amount of tensile strain (0.15%) measured under same conditions yields a ~8 mV smooth V_{oc} drop. Both V_{oc} changes were found exactly synchronized with stains.

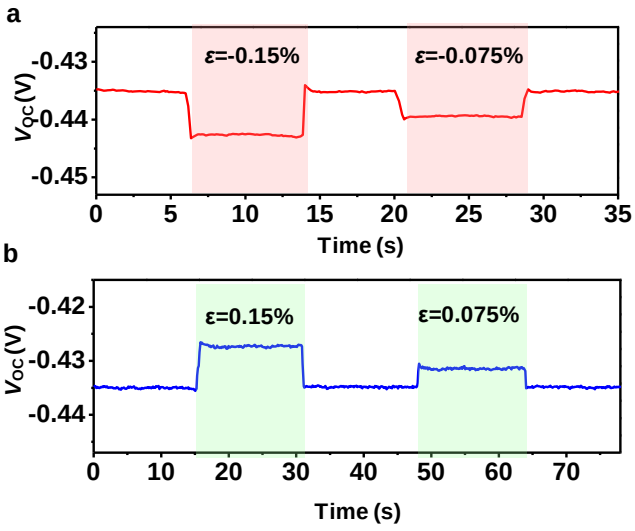

Figure S6. Potentiostat measurements of open circuit voltage change of a ZnO/PbS QDSC under different constant strains.

S6. Open Circuit Voltage versus Short Circuit Current

To quantify the V_{oc} shift purely from J_{sc} change, we collected the *J-V* characteristics of the QDSC under different intensities of light illuminations (Fig. S7a). It is known that V_{oc} is a logarithm function of J_{sc} as shown in equation (4) in the main text. To obtain the prefactor *nkT/e*, V_{oc} and ln(J_{sc}) are plotted together and the data set was fitted by a straight line (Fig. S7b). The slope of the fitted line, *nkT/e*, was calculated to be 40 mV, and the ideal factor, *n*, was found to be 1.55. These values were comparable to the reported value.[4] With this calibrated data, we could compute the change of V_{oc} merely from J_{sc} change and distinguish it from the V_{oc} change as a result of remnant polarization on the ITO-ZnO side.

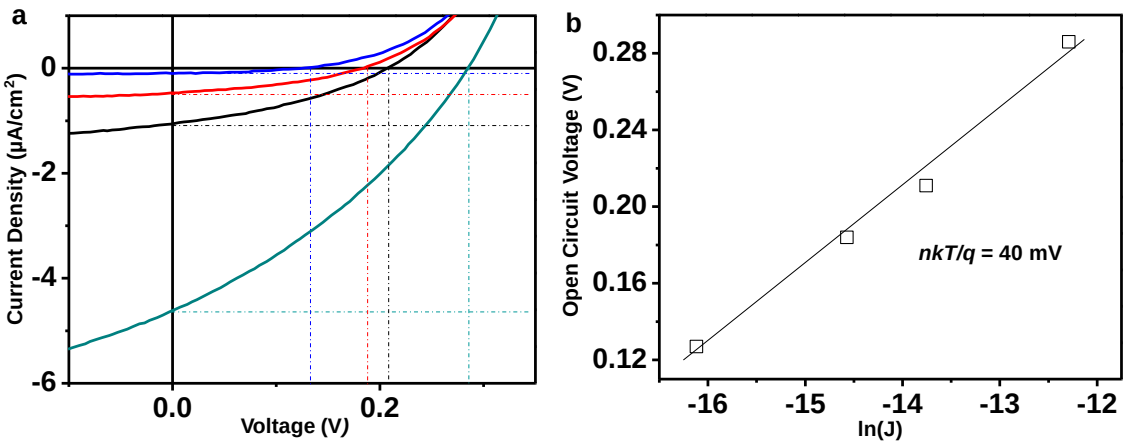

Figure S7. A. J-V characteristics of solar cells under different illumination intensities for calibrating. **B.** the open circuit voltage change merely induced by short circuit current change.

S7. QDSC Performance under High-Intensity Illumination

Strong illumination can significantly increase the effective charge carrier concentration ($N_{PbS,\mathrm{eff}}$) at the ZnO/PbS interface, which diminishes the P_{pz}-induced expansion of depletion region. Therefore, the QDSC measured under 100 mW/cm^2 was nearly nonresponsive to P_{pz}. The *J-V* curves kept nearly the same shape when the QDSC was under ±0.15% tensile and compressive strains (Fig. S8a). Particularly, the J_{sc} appeared independent to the applied strain, *i.e.* P_{pz}, and remained a constant 6.57 mA/cm^2 (Fig. S8b). The constant J_{sc} evidenced that the P_{pz} had negligible effect on charge extraction when incident light intensity was high enough. Although no J_{sc} change was observed, small changes of V_{oc} during straining were still obtained, which was ∓ 8 mVs with $\pm 0.2\%$ strain (Fig. S8c). The shift direction of the V_{oc} was identical to the band structure illustrated in Fig. 4b. Under this situation, the V_{oc} change was not related to J_{sc} and solely contributed by the remnant piezopotential at the ITO/ZnO interface, $\Delta\varphi_{\mathrm{pz,r}}$.

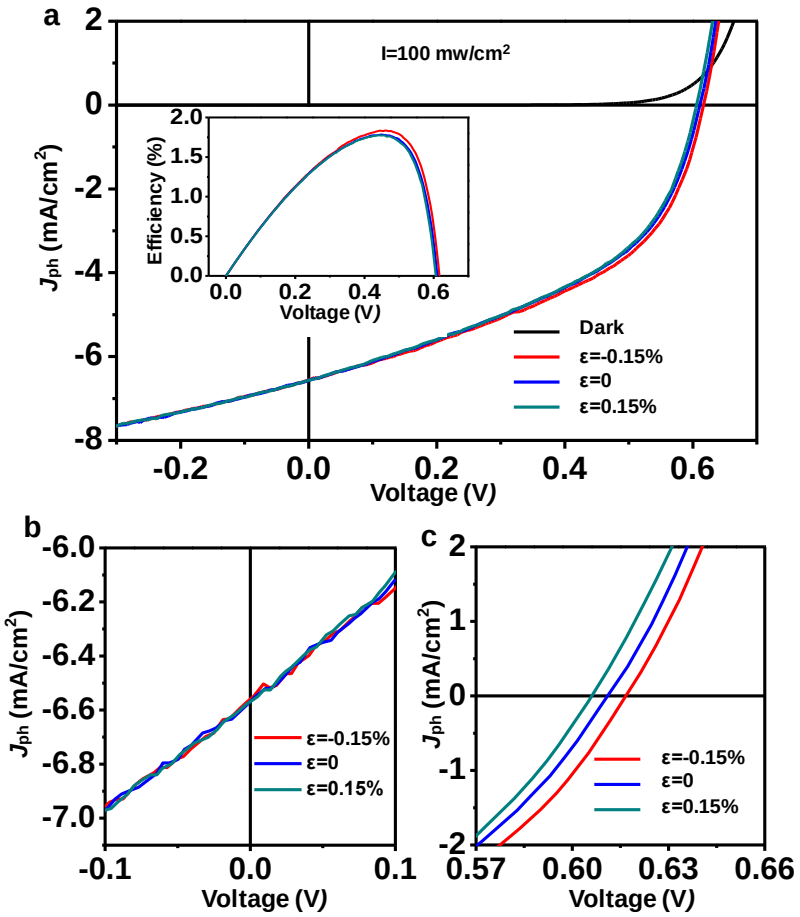

Figure S8. P_{pz}-modulated Performance of QDSC under strong illumination. a, *J-V* characteristics of the QDSC under 100 mW/cm^2 illumination, when the cell subjected to zero and ±0.15% strain. Inset shows the calculated efficiencies. **b,** Plot at *V*=0 region illustrates that J_{sc} did not change under appreciable strain (±0.15%). **c,** Plot at *J*=0 region illustrates the slight changes of V_{oc} in response to strain.

References

[1] N.W. Ashcroft, N.D. Mermin, Solid State Physics (Saunders College Publishing, New York, 1976)

[2] P. Wurfel, I.P. Batra, Phys. Rev. B 8, 5126 (1973).

[3] J. Bisquert, G. Garcia-Belmonte, A. Munar, M. Sessolo, A. Soriano, and H. J. Bolink, Chem. Phys. Lett. 465, 57 (2008).

[4] S. M. Sze, K. K. Ng, Physics of Semiconductor Devices (Wiley, New Jersey, 2007).

[5] S.M. Willis, C. Cheng, H.E. Assender and A.A.R. Watt, Nano Lett. 12, 1522 (2012).

[6] Ü. Özgür, Ya. I. Alivov, C. Liu, A. Teke, M. A. Reshchikov, S. Doğan, V. Avrutin, S.-J. Cho, and H. Morko ç J. Appl. Phys. 98, 041301 (2005).

[7] I. Moreels, D. Kruschke, P. Glas and J.W. Tomm, Opt. Mater. 2, 496 (2012).